The source regions of whistlers

Dávid Koronczay[1,2], János Lichtenberger[1,2], Mark A. Clilverd[3], Craig J. Rodger[4], Stefan I. Lotz[5], Dmitry V. Sannikov[6], Nina V. Cherneva[6], Tero Raita[7], Fabien Darrouzet[8], Sylvain Ranvier[8], Robert C. Moore[9]

[1]Department of Geophysics and Space Sciences, Eotvos University, Budapest, Hungary
[2]Research Centre for Astronomy and Earth Sciences, Hungarian Academy of Sciences, Sopron, Hungary
[3]British Antarctic Survey (NERC), Cambridge, UK
[4]Department of Physics, University of Otago, Dunedin, New Zealand
[5]Space Science Directorate, South African National Space Agency, Hermanus, South Africa
[6]Institute of Cosmophysical Research and Radio Wave Propagation, Far Eastern Branch of the Russian Academy of Sciences, Paratunka, Russia
[7]Sodankylä Geophysical Observatory, University of Oulu, Oulu, Finland
[8]Belgian Institute for Space Aeronomy, Brussels, Belgium
[9]Department of Electrical and Computer Engineering, University of Florida, FL, USA

Key Points:

- We present a method for identifying the geographical source regions of lightning generated whistlers.
- Whistler source regions corresponding to 15 fixed whistler detector ground stations are determined.
- Whistler transmission rates as a function of location are also determined.

Corresponding author: David Koronczay, `david.koronczay@ttk.elte.hu`

Abstract

We present a new method for identifying the source regions of lightning generated whistlers observed at a fixed location. In addition to the spatial distribution of causative lightning discharges, we calculate the ratio of lightning discharges transmitted into ground detectable whistlers as a function of location. Our method relies on the time of the whistlers and the time and source location of spherics from a global lightning database. We apply this method to whistlers recorded at fifteen ground based stations in the AWDANet (Automatic Whistler Detector and Analyzer Network) operating between 2007-2018 and to located lightning strokes from the WWLLN (World Wide Lightning Location Network) database. We present the obtained maps of causative lightning and transmission rates. Our results show that the source region of whistlers corresponding to each ground station is around the magnetic conjugate point of the respective station. The size of the source region is typically less than 2000 km in radius with a small fraction of sources extending to up to 3500 km. The transmission ratio is maximal at the conjugate point and decreases with increasing distance from it. This conforms to the theory that whistlers detected on the ground propagated in a ducted mode through the plasmasphere and thus the lightning strokes of their causative spherics must cluster around the footprint of the ducts in the other hemisphere. Our method applied resolves the whistler excitation region mystery that resulted from correlation-based analysis methods, concerning the source region of whistlers detected in Dunedin, New Zealand.

1 Introduction

Whistlers are very low frequency (VLF) electromagnetic waves originating from lightning discharges. These waves can penetrate into and through the ionosphere, entering the magnetosphere. They take a specific time-frequency shape through propagating in a dispersive medium, which is the magnetospheric plasma surrounding the Earth (Helliwell, 1965). Some of these waves may be trapped in field aligned density plasma irregularities, or ducts, extending between the two hemispheres. The trapping mechanism is explained by the theory of Smith et al. (1960). Smith (1961) lists evidence of the existence of ducts of enhanced density and describes whistler propagation in this structure. The ducts guide the whistlers to the magnetic conjugate point, where, given the right conditions, they can re-enter through the ionosphere and become detectable on the ground in the conjugate hemisphere. Another significant portion of the signals remain non-ducted.

Lightning generated whistlers are known to significantly affect the radiation belts through wave-particle interactions, causing acceleration (Trakhtengerts et al., 2003) and losses, be it oblique or magnetospherically reflected whistlers (Lauben et al., 2001; Bortnik et al., 2006) or ducted whistlers (Helliwell et al., 1973; Rodger et al., 2004). This whistler induced precipitation in turn influences the ionosphere (Helliwell et al., 1973; Rodger et al., 2007). It has been shown that most lightning generated spherics leak into the ionosphere (Holzworth et al., 1999) and during strong lightning activity a significant fraction will reach the equatorial magnetosphere as whistlers (Zheng et al., 2016). They substantially affect the overall wave intensity in this region at the relevant frequencies (Záhlava et al., 2018). The shape of the whistler signals carry information on the magnetospheric plasma and has been used to investigate the plasmasphere (Helliwell, 1965; Park, 1972; Carpenter, 1988; Lichtenberger et al., 2013). Specifically, they serve as a ground based tool for mapping electron densities in the plasmasphere (Park et al., 1978). The detection and analysis of these waves have recently become a fully automated operation (Lichtenberger et al., 2008, 2010). The fact that whistlers are used as a remote sensing tool to study the plasmasphere and their role in controlling radiation belt populations provide a motivation to better understand their source and propagation.

The conditions for VLF signal propagation into the magnetosphere are better at high geomagnetic latitudes (Helliwell, 1965), while lightning occurs predominantly in the tropics, at low geographic latitudes (Christian et al., 2003). Thus, the resulting long term whistler rate at any location is a result of the two effects. Evidence suggests that there exists a low-latitude cutoff at geomagnetic latitude 16° below which no whistlers can be observed on the ground, either due to a lack of appropriate trapping and transmission conditions or a lack of ducts (Rao et al., 1974; Helliwell, 1965). Furthermore, there are a number of variable conditions that can influence the transmission of whistlers to the ground, such as lightning activity at any given time, ionospheric conditions, the presence of ducts, etc. The occurrence rate of whistlers is generally much lower than the rate of conjugate lightning discharges. Thus, it is of interest to know which factors determine the reception of whistlers. Since lightning remains a source effect, understanding its role is a necessary first if we are to untangle these various factors.

While the general picture of whistler propagation is understood, the exact location and extent of the source region is unknown. A natural assumption is that the source is symmetrically centered on the conjugate point, but this has not been demonstrated. Yoshino (1976) found that lightning activity was displaced poleward and west from the conjugate point of Sugadaira, Japan, while Öster (2009) observed the source lightning distribution extending poleward and east from the conjugate point of Tihany, Hungary. Gokani et al. (2015) observed a similar tendency for source lightning corresponding to very low latitude whistlers observed at Allahabad, India. While the propagation mechanism of very low latitude whistlers is not well understood, they showed the likely source region to be within 1000 km radius of the conjugate point. Whistlers have been associated with lightning strokes occurring at 2000 km from the duct footprint by Storey (1953), 2500 km by Carpenter and Orville (1989) and, in the case of whistlers at polar latitudes, several thousand km by Allcock (1960). Such propagation paths for whistler-mode waves were confirmed by Clilverd et al. (1992). We note that even for whistlers that are eventually trapped in ducts, a part of the path in the ionosphere and magnetosphere may be non-ducted. According to a review by Holzworth et al. (1999), upward going whistlers can be detected in the ionosphere at over 1000 km horizontal distance from the lightning sources, based on rocket experiments. Chum et al. (2006) manually identified 3500 fractional hop whistlers on the DEMETER satellite in low Earth orbit and paired them to lightning strokes from the EUCLID (European Cooperation for Lightning Detection) regional database, finding that lightning discharges enter into the magnetosphere as whistler mode waves at distances up to 1500 km from the source.

An example of the holes in our understanding of whistler sources is the "Dunedin paradox". Lightning rate at the corresponding conjugate point is orders of magnitude lower than the whistler rate observed in Dunedin, New Zealand. In addition, the time of the daily peak of the whistler rate at Dunedin is in disagreement with the peak of lightning activity at the conjugate point (Rodger, Lichtenberger, et al., 2009). The results of Collier et al. (2010) suggest tropical Mexico, over 7000 km from the conjugate point, as the source region, which, however, seem to contradict our understanding of the fundamental physics and also other observations (Morgan & Allcock, 1956; Antel et al., 2014).

Apart from the direct matching of a small number of whistlers to lightning discharges, as done by Storey (1953); Allcock (1960); Carpenter and Orville (1989), there have been few more general correlation studies. Ohta and Hayakawa (1990) found no correlation between whistler rates at Yamaoka, Japan, and lightning flash rates at the vicinity of its conjugate point in Australia. Whistler measurements were done between 1 to 15 January of every year from 1977 to 1987; while only monthly flash counts were available in the conjugate area, within a 50 km range, providing a limited dataset. Collier et al. (2006) compared the diurnal and seasonal rate of whistlers observed at a mid-latitude station (Tihany, Hungary, L=1.8) and the lightning activity in the assumed source region based on data from WWLLN and LIS/TRMM (Lightning Imaging Sensor on the Tropical Rainfall Measuring Mission satellite), with results broadly consistent with expectations.

Collier et al. (2009) presented a method of calculating Pearson correlation coefficients between whistler rates and lightning rates separately for each of the grid cells spanning the globe. They applied this method to whistlers recorded at Tihany station, Hungary, between 1 January 2003 and 19 May 2005. The results showed significant positive correlation near the conjugate point of the station within a $\sim$1000 km radius, especially in the afternoon and early night. Collier et al. (2010) applied the same method to whistler series from Dunedin, New Zealand, recorded between 20 May 2005 and 13 April 2009. In this case, the results showed a lack of correlation in the vicinity of the conjugate point (near Alaska Peninsula), weak correlation over the North Pacific, and strong correlation in Mexico. Since the Pearson correlation coefficient is sensitive to large spikes that are often present in lightning discharge rates, Collier et al. (2009, 2010) used a boolean rounding, collating event counts within a predetermined time slot ($\Delta t = 1$min) to 0 or 1 to overcome this problem, at the cost of losing some amount of information. In a subsequent study by Collier et al. (2011) of whistlers recorded at Rothera, Antarctica, between 13 May 2008 and 30 December 2009, no such reduction was applied to the event rates. In this case, significant positive correlation over the Gulf stream, an active lightning center near the conjugate point of Rothera, was observed. In all of the studies mentioned (Collier et al., 2009, 2010, 2011), the method lead to other, additional areas of positive correlation, far away from the conjugate points, that may or may not be actual sources. A similar study by Vodinchar et al. (2014) analysed whistlers detected at Karymshina, Kamchatka, between 1 to 11 March 2013 and 1 to 30 September, 2013. In addition to Pearson correlation coefficients with boolean rounding, their analysis applied Spearman rank correlation coefficients to the real (unrounded) whistler time series and lightning time series calculated for each continent. No significant positive correlation was found near the conjugate point of the station, or in surrounding Australia in general.

Collier et al. (2011) also present another, different method for mapping causative lightning strokes. Instead of relying on correlations, this direct method simply registers every lightning stroke that falls within a predetermined time window preceding each whistler recorded at a specific ground station, Rothera, in this case, and the geographic distribution of those lightning strokes are presented on a density map. The results show a strong reminiscence of the lightning density distribution around the Gulf Stream, an area with high frequency of lightning, leading to a much more well defined result than those of the correlation-based methods listed above.

The goal of our paper is a better understanding of the positions of causative lightning strokes that lead to whistlers. Once the source regions are reliably identified, subsequent studies can look into correlations between whistler counts and lightning in the source region. With the availability of long-term global lightning data through WWLLN, and our large dataset of AWDANet whistler measurements from fifteen stations around the world recorded over twelve years, we can extend our investigation into a significantly larger scale than previous studies.

2 Data

The WWLLN (World Wide Lightning Location Network, http://www.wwlln.com/) is a global network consisting of VLF sensors. The network uses the time of group arrival method from at least five stations to locate individual lightning strokes. Due to the low attenuation of VLF waves in the Earth-ionosphere waveguide, it has global sensitivity, as opposed to regional lightning detector networks often operating at higher frequencies. A temporary drop-out of any single station has only a slight effect on the detection efficiency (Hutchins et al., 2012). Therefore, the lightning stroke time series used in this study was considered continuous, without any data gaps.

The number of stations in the network steadily increased from 23 stations in 2005 to $\sim$70 stations at present. After the upgrades in the processing algorithm (used to reprocess the entire raw dataset), this expansion resulted in the total number of located lightning strokes of 36 million in the year 2005 increasing to 208 million by 2017. WWLLN is capable of detecting both cloud-to-ground (CG) and intracloud (IC) flashes of sufficient strength. The total detection efficiency (CG+IC) is estimated to have increased from 2.6% in 2005 to about 15% in 2017 (Rodger et al., 2006; Rodger, Brundell, et al., 2009; Abarca et al., 2010; Rodger et al., 2014). In addition, detection efficiency is strongly dependent on peak current, and can be as high as 35% for currents exceeding −130kA (Abarca et al., 2010). Detection efficiency in the long term is lowest over ice covered surfaces such as Greenland and Antarctica (Hutchins et al., 2012). Location accuracy is estimated at < 10km, much smaller than the pixel sizes on Figures 2-9. In the present study we used 2×10^9 lightning strokes with locations from WWLLN, recorded between 2007 and 2018.

Table 1. Whistler recordings processed in this study, in regional grouping

Station	Geodetic coordinates	L-value[a]	Years processed	Total number of whistlers	Max. transmission rate [%]
Dunedin	45.7°S, 170.5°E	2.78	2007-2017	3,660,000	75
Karymshina	53.0°N, 158.7°E	2.18	2012-2016	3,110,000	25
Palmer	64.8°S, 64.0°W	2.52	2009-2010	17,600,000	50
Rothera	67.5°S, 68.1°W	2.82	2008-2016	43,300,000	20
Halley	75.6°S, 26.6°W	4.75	2012-2015	4,300,000	30
SANAE	71.7°S, 2.8°W	4.60	2006-2016	1,780,000	20
Sutherland	32.4°S, 20.6°E	1.78	2007-2011	30,000	0.5
Grahamstown	33.3°S, 26.5°E	1.82	2015-2018	124,000	0.5
Marion Island	46.9°S, 37.9°E	2.68	2009-2016	3,540,000	12
Tihany	46.9°N, 16.9°E	1.83	2007-2017	820,000	4
Gyergyóújfalu	46.7°N, 25.5°E	1.84	2007-2016	120,000	2
Nagycenk/Muck	47.6°N, 17.7°E	1.81	2007-2018	285,000	3
Humain	50.2°N, 5.2°E	2.09	2011-2018	128,000	4
Eskdalemuir	55.3°N, 3.2°W	2.72	2011-2018	10,000	≥ 12
Tvärminne	59.8°N, 23.0°E	3.32	2013-2018	346,000	≥ 15

[a]At 100 km altitude and at the epoch of 2015 using the IGRF-12 geomagnetic model (Thébault et al., 2015).

The AWDANet (Automatic Whistler Detector and Analyzer Network) is a global ground-based network of VLF stations that automatically detect and analyze whistlers (Lichtenberger et al., 2008). In the first data processing segment, the detection of whistlers yields a time series of whistler traces. The second segment, the analysis involves the scaling and inversion of each whistler signal, and yields plasmaspheric electron densities along the propagation field line, the L-value of the field line, and an estimation of the time of the originating lightning stroke (Lichtenberger et al., 2010). While the latter can be of help when associating causative strokes to whistlers, currently only about 1 to 5% of the input is successfully inverted by the algorithm, significantly reducing the statistics. Therefore, we chose to use the results of only the detector segment, the time series of whistler traces. We note that both networks use GPS timing, and the time accuracy of AWDANet whistlers is limited by the spread of the whistler traces to ~ 1 ms, while the accuracy of the reconstructed time of lightning strokes in WWLLN is $\ll 1$ ms.

AWDANet has been in real-time operation providing prompt results since 2014. To extend this dataset, we have also processed available raw data between 2007 and 2014. The earlier (2002-2007) measurements were not based on GPS precision timing and therefore we excluded those from the analysis. Nevertheless, our method should in principle work with less accurate times, too. Table 1 lists the detector stations in regional groupings, the years of observations processed, and the total number of whistlers. Altogether we used 77 million whistler traces in this study from the fifteen stations combined. Finally, the last column of the table shows the so-called maximal transmission rate, or the ratio of lightning in the source region that is transmitted into whistlers, a result of the calculations explained in subsection 3.2. Note that the number of whistlers observed, and as a consequence the transmission rate, too, is sensitive to the local noise at the station.

In addition to AWDANet stations, data from Palmer Station, Antarctica are also included in this report. The VLF system at Palmer Station consists of two orthogonal IGY loop antennas with a sensitivity of 5.7×10^{-18}THz$^{-1/2}$ at 10 kHz. The frequency response of the Palmer VLF system is flat between 130 Hz and 45 kHz, and data are recorded continuously at 100 kHz with 16-bit precision. Timing is supplied by a GPS-trained oscillator with 10^{-12} frequency precision.

3 Method

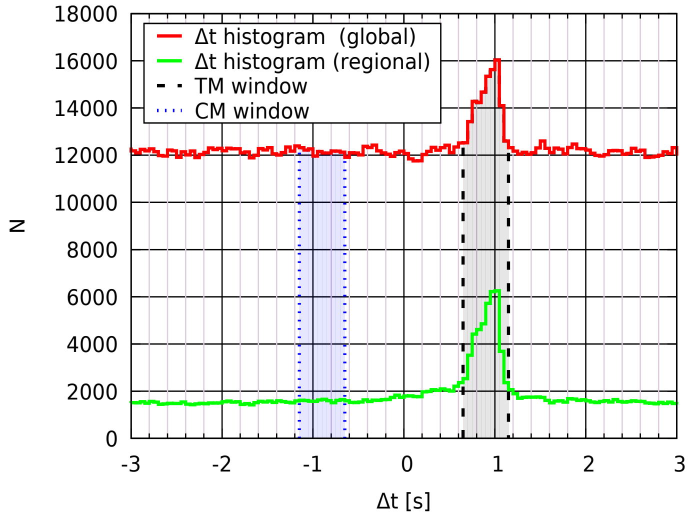

Figure 1. Histogram of time differences between whistlers and lightning strokes, using WWLLN global data (red) and data restricted to the conjugate region (green). $\Delta t = t_{\text{whistler}} - t_{\text{lightning}}$, while N is the number of lightning-whistler pairs. The peak is due to the tendency of whistlers to occur after causal lightning, while the background is caused by chance matches between unrelated whistlers and lightning. The peak is much more prominent on the regional map. Black dashed lines represent a time window for the selection of source strokes (TM, total matches). Blue dotted lines show a window of identical length (CM, chance matches) but with whistlers preceding lightning strokes to exclude any causality, used for the statistical removal of chance matches. This example was computed from data received at Nagycenk station.

Correlation-based methods described in the Introduction have a number of weaknesses. First, the resulting correlation maps sometimes include areas of negative correlation that have no relevant physical meaning. Second, more importantly, areas of positive correlation do not necessarily imply causality. For example, it is conceivable that the diurnal variation of the lightning flash rate at one location is, simply by chance, similar to the diurnal variation of the whistler rate at another location, the latter arising from a combination of source lightning flash rate, diurnal ionospheric changes and other propagation effects in the ionosphere and the plasmasphere, leading to some level of positive correlation between the two. Thirdly, by the same logic, any real positive correlation between whistlers and causative lightning strokes may be damped by time dependent propagation effects between the source and the detection.

For this reason, instead of relying on perceived correlations, we focus on the direct method, explained in Collier et al. (2011) as a second method. This procedure attempts to directly pair up whistlers with their corresponding source lightning based solely on their timing. In an additional step we statistically correct for false matches, as explained in the next section.

3.1 Mapping causative lightning strokes

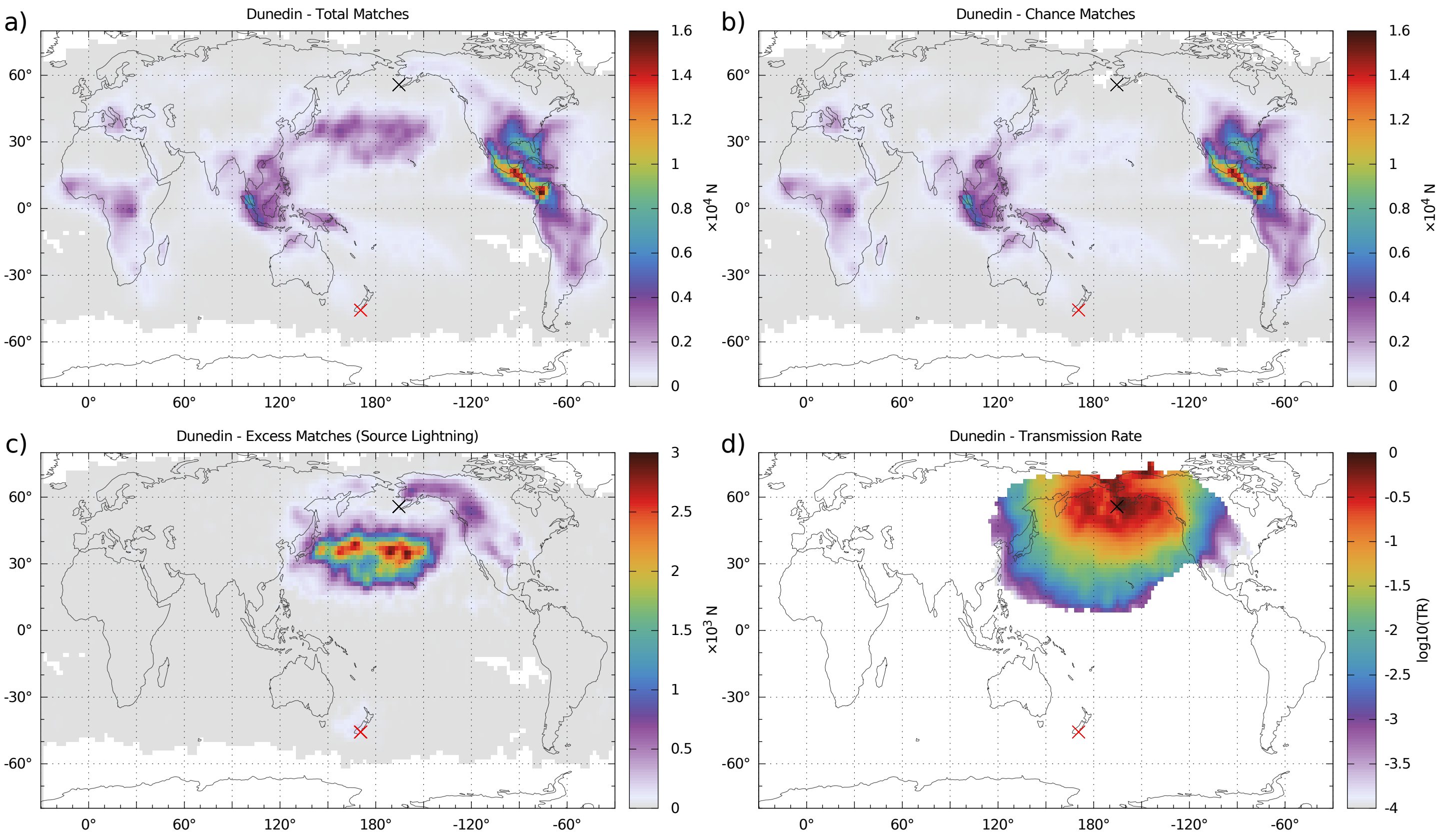

Figure 2. Demonstration of the steps of our method. (a) Total matches (TM): distribution of all lightning strokes in the positive time window (lightning preceding whistlers, see Figure 1) Pixel size is 2° × 2°, color represents the number of matched strokes (N) in the given pixel. (b) Chance matches (CM): distribution of lightning activity in the negative time window (lightning following whistlers, excluding causality, representing purely chance matches between the two). (c) Excess matches (EM): difference between TM and CM. (d) Transmission rate (TR), or the number of excess strokes divided by the climatology shown in Figure 3, or the total number of WWLLN lightning strokes over the same time period. Transmission rate (R) is shown only in the area of significant source lightning. All maps are smoothed using a 3 × 3 pixel Gaussian kernel. The red cross marks the location of the whistler recording station, the black cross marks its geomagnetic conjugate point using the IGRF-12 geomagnetic field model (Thébault et al., 2015).

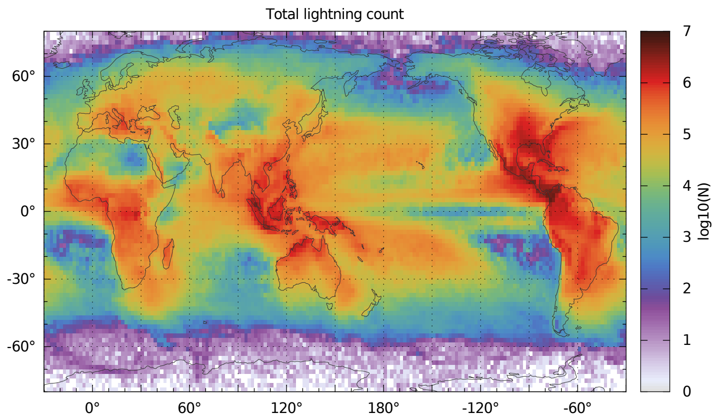

Figure 3. "Climatology", or total number of WWLLN lightning strokes over the entire measurement period of the whistler station in question (Dunedin, 2007-2017). Periods when the whistler recording station was offline were excluded. Such maps are used for the normalization of lightning source maps to produce transmission rate maps, an example of which is shown in Figure 2d. Pixel sizes are same as for Figures 2a-2d, $2^\circ \times 2^\circ$. Pixel colours represent absolute number of located lightning discharges within the pixel, without correction for pixel sizes varying with latitude. Apart from this latitudinal factor, this map is similar to lightning density climatologies normalized to flashes $\mathrm{km}^{-2}\ \mathrm{yr}^{-1}$, see e.g. the lightning climatology obtained from WWLLN on Figure 2b in Virts et al. (2013).

The only adjustable parameter in the direct technique is the time window prior to each whistler in which lightning strokes are considered. This should be different for every station and is thus set separately for each one. In theory, a practical time window could be calculated as the minimum and maximum travel times of the source spheric travelling along the field line, depending on possible values of plasmaspheric density and field line L-value. Since there are no sharp limits on these values, we instead experimentally determine the appropriate time window from the data. Given a list of n whistler times and m lightning times, first an $n \times m$ matrix is computed of every possible time difference between whistlers and lightning strokes, such that the value of matrix element M_{ij} is the $t_{\mathrm{whistler}_i} - t_{\mathrm{lightning}_j}$ difference of the time of the i-th whistler and the j-th lightning. Next, an occurrence histogram of the time differences in the matrix is computed. (A similar construct was used earlier by Chum et al. (2006).)

Figure 1 shows such a histogram, with a time bin of 50 ms, limited to practical values of a couple of seconds around zero time difference. If the two time series were independent, the time differences would be distributed randomly and uniformly on the histogram. The peak in the distribution is due to the fact that whistlers tend to occur a short time after their causative spheric, with the peak location corresponding to the most common travel time from the source through the magnetosphere to the location where it is recorded by a ground station. Based on the location and width of the peak an appropriate window of a few hundred millisecond was determined for each whistler detector station separately.

Next, we create a series of density maps. The first map represents the matched lightning strokes. For each grid cell on a geographic map, the total number of WWLLN strokes occurring within the predetermined time window preceding a whistler is calculated and the value is assigned to the cell. The obtained map of total matches, (TM, see Figure 2.a for the TM map for Dunedin) should contain the actual source lightning strokes, but also a lot of chance coincidences, especially in regions of intense lightning activity. In order to remove these chance coincidences from the map, we try to estimate their expected value. Naturally, at locations of high lightning activity, such as the three main tropical lightning centers (visible on Figure 3 representing long-term lightning activity), the probability of chance coincidences is higher, explaining some of the patches on Figure 2.a. A static map of lightning activity, however, cannot be directly used for the estimation of chance matches, since both whistler and lightning rates exhibit strong diurnal and seasonal variations, necessitating a combination appropriately weighted seasonal and hourly climatologies. Instead of such a complicated procedure, we simply calculate matches between lightning strokes and whistlers in another time window, representing the "background noise". By choosing a window (see Figure 1) that corresponds to negative time difference between whistlers and lightning strokes, we can be sure that no causative strokes are included in the selection. For each event, this window for background noise calculation precedes the other window by merely a few seconds, which ensures that the global lightning activity and thus the likelihood of chance matches do not deviate significantly from that within the other (causative) window. Detection efficiency of whistlers and spherics should also remain constant over such short period of time. Figure 2.b shows the density map of chance matches (CM) calculated this way, again for the Dunedin station.

Finally, we subtract the two density maps to obtain a map representing only the excess matches (EM): EM = TM − CM. Since these excess matches are due to the causative lightning strokes, the obtained map represents the geographic distribution of the causative lightning strokes corresponding to the whistlers detected at the given ground station. We term these "source lightning".

Remarkably, in the above procedure, there was no input specifying where the whistler time series was recorded, we simply used the Dunedin whistler time series as observed. Nevertheless, the resulting map on Figure 2c clearly shows the source lightning distribution surrounding the conjugate point of Dunedin, New Zealand. This correspondence repeats when we undertake these calculations for each of the fifteen AWDANet stations, a strong validation of our method. Note that the colour scale in Figure 2c is ∼5 times smaller than that of Figures 2a and 2b. This emphasises the large number of chance matches, and also demonstrates how the chance matches can so easily lead to misleading results when simple correlation approaches are used.

3.2 Mapping whistler transmission rates

The procedure described so far tells us where the lightning source regions corresponding to a given whistler recording station are located. We can also calculate the geographic distribution of an additional parameter, the ratio of lightning transmitted into whistlers. The low absolute number of source lightning in the vicinity of the conjugate point of Dunedin, for example, is not in itself surprising given the fact that the region shows very limited lightning activity in general. This motivates a normalization of the source lightning counts with the total population of lightning strokes. Figure 3 shows an example of the latter, a "climatology" (CL) calculated as the total number of WWLLN lightning strokes over the period under study when the AWDANet station in question was in operation. Periods of data gaps in the whistler data (due to instrumental problems, data loss, etc.) are excluded from the count. This is the lightning stroke population which could theoretically generate the whistlers present in the time series. Note that all of the maps on Figures 2, 3 and 4 were calculated using $2^\circ \times 2^\circ$ geographic grid cells.

Dividing the source lightning count (obtained by the procedure described in Subsection 3.1) by the total lightning population over the same time period, we obtain a so-called transmission rate, or the percentage of lightning strokes that generated whistlers observable at the relevant station. By doing so for each grid cell of the two maps (excess matches and climatology), this transmission rate (TR) can also be represented on a density map: TR = EM / CL. Figure 2.d shows an example of the results obtained by this procedure, again for the Dunedin AWDANet station. The transmission rate is calculated only for pixels with significant source lightning levels.

To a first approximation, the obtained TR is insensitive to the varying detection efficiency of the WWLLN network, since both the source lightning and the total lightning counts should be affected similarly. However, it is possible that the sub-population of lightning strokes capable of whistler generation have different detection efficiency. WWLLN detection efficiency depends on the lightning peak current, for example, which may affect whether an observable whistler is generated.

The whistler detection efficiency of AWDANet is also difficult to ascertain. Our preliminary study (Lichtenberger et al., 2008) showed that the whistler detector trace finder at the Tihany station works at $< 3\%$ false positive and $< 5\%$ false negative detection rate. Nevertheless, unlike with lightning detection networks, we cannot compare our measurements to independent datasets. The aforementioned detection rate estimates are based on the assumption that whistler traces on the spectrograms recognized by the human eye constitute the total population of whistlers. Clearly, this is not necessarily true, as some traces, especially those having smaller amplitudes, may be swamped by noise in the same frequency band. How many traces are lost to the noise is not known. In our experience, the local electromagnetic noise levels of both artificial and natural origin are different at each station, and can be strongly time dependent.

Thus, the level of completeness of both time series is difficult to ascertain. Therefore, the obtained TR should be taken as relative values, not necessarily directly comparable between stations.

4 Results

The procedure described in Section 3 is repeated for each station. Figure 4 shows the source lightning distribution and transmission rates for four stations, located in four different regions across the globe. These (and Figures 2c-2d) demonstrate that the lightning which are whistler sources lie within a few thousand kilometers of the geomagnetic conjugate point, as expected. No sources or discernible transmission rate can be observed outside this area. The global lightning centers in the tropics play little to no role in the generation of ground detectable whistlers, at least for these middle to lower middle latitude stations, due to their large distance from these latitudes.

Having established a global picture, the following maps are limited to the conjugate region for better viewing. Figures 5 to 9 are in azimuthal equidistant projection, which keeps true great circle distance and azimuth from the center point, the conjugate point of the relevant whistler detector station. Also, this projection has little areal distortion within a few thousand kilometers of the center point. We used 200×200 km pixels and applied a 3×3 Gaussian smoothing kernel to each map. Three concentric circles are plotted around the conjugate points, representing distances of 1000, 2000 and 3000 km. For better comparison, we used the same coordinate ranges and in the case of the transmission maps the same logarithmic scale for each map.

The maps are presented in regional groups. The top panels of Figure 5 show the source lightning distribution (EM) and transmission rate (TR) of whistlers detected at Dunedin, New Zealand, at its conjugate area located near Alaska. The bottom panels of Figure 5 are the same for whistlers detected at Karymshina, Kamchatka, with the conjugate area being located near Australia. Figure 6 shows conjugate areas in North America corresponding to stations in West Antarctica: Palmer, Rothera, Halley and SANAE. Figure 7 shows conjugate areas in Europe corresponding to stations in Southern Africa: Sutherland, Grahamstown and Marion Islands. Figure 8 shows conjugate areas in Southern Africa corresponding to the European stations of Humain, Eskdalemuir and Tvärminne. Finally, Figure 9 shows the source lightning and transmission rate distribution for fur-

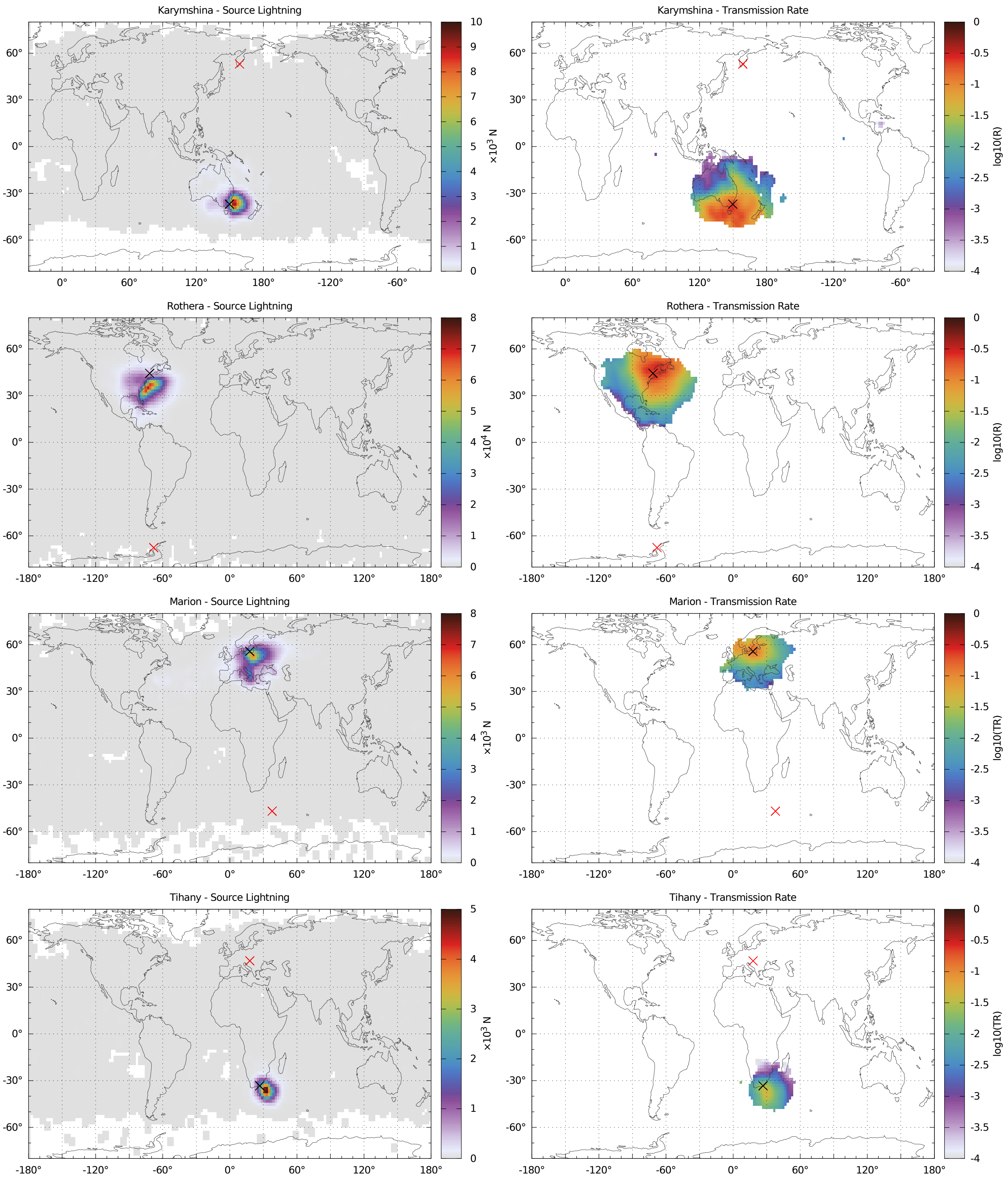

Figure 4. Distribution of source lightning (EM, left) and transmission rate (TR, right) on a global map, in four regions. The left hand panels are in the same format as Figure 2c, while the right hand panels are in the same format as Figure 2d.

ther three, closely separated stations in Central Europe: Nagycenk/Muck, Tihany and Gyergyóújfalu.

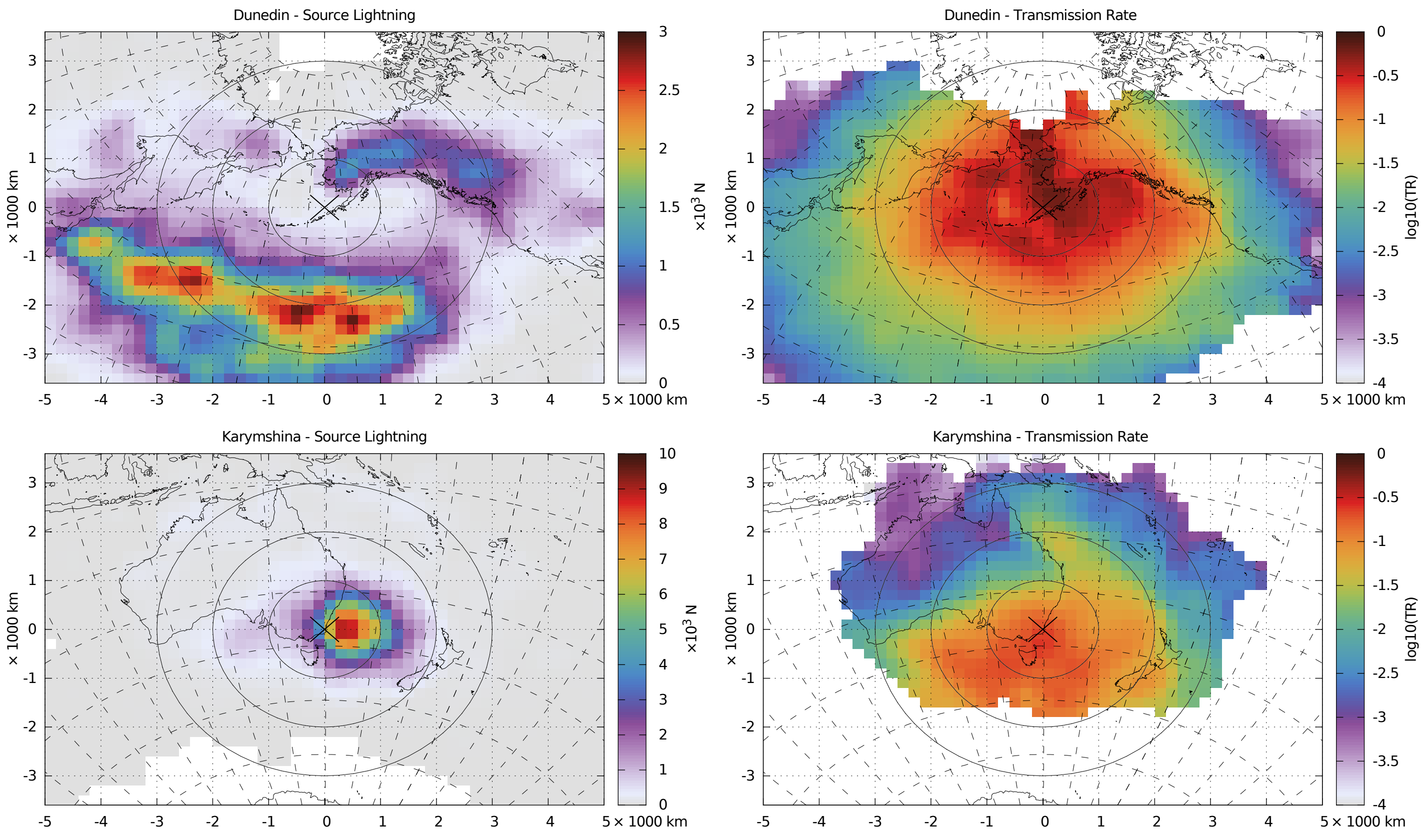

Figure 5. (top) Regional distribution of source lightning (EM) and transmission rate (TR) for whistlers detected at Dunedin, New Zealand (showing its conjugate region near Alaska). (bottom) Same for Karymshina, Kamchatka (showing its conjugate region near Australia). The concentric circles represent distances of 1000, 2000 and 3000 km from the conjugate points.

5 Discussion

The regional maps show that the source lightning distribution is dominated by the nearest conjugate region of high lightning activity. This is in agreement with the similar conclusion of Collier et al. (2011) based on the second method listed there. Our method, however, does not produce any stray regions of whistler sources away from the conjugate region, unlike the first method of Collier et al. (2011). In some cases, the majority of the source lightning can be significantly offset from the actual conjugate point, such as in the case of Rothera, Halley and SANAE (where lightning above the Gulf current dominates), or Dunedin (where patches in the North Pacific Ocean dominate). The transmission maps, however, do not show such offsets in the distribution, and instead the transmission rate decreases largely monotonously with increasing distance from the conjugate point. The transmission rate is largest at or near (within 1000 km) of the conjugate point. No significant poleward offset can be observed in the distribution of the transmission rate. Nevertheless, such an offset cannot be entirely excluded, since in many cases, the poleward parts of the distribution are missing due to very low lightning activity at high latitudes. Also, the AWDANet whistler detector was optimized for whistlers with $L < 4.5$ and thus some part of the population may be missing.

The maps on the top panel of Figure 5 seem to partially answer the "Dunedin paradox" (Rodger, Lichtenberger, et al., 2009). The immediate area of the conjugate point of Dunedin indeed exhibits very low lightning activity. Nevertheless, as the transmission rate map shows, a large number of lightning discharges from further away will find their way to Dunedin, albeit with decreasing efficiency as we get further from the conjugate point.

In some cases (Palmer, Rothera, Halley, SANAE, see Figure 6, and Dunedin, see Figure 5), significant levels of transmission rate extend over 3000 km. On the other hand, the maximal transmission rate, and possibly as a consequence, the geographical extent seems to be small at low latitude stations, such as Humain, Tihany, Gyergyóújfalu, Nagycenk/Muck, Grahamstown and Sutherland. It is not known, how much of this is a result of lower detection efficiency at these stations due to local noise conditions.

Finally, we note that in some cases, there is a hint of land/sea asymmetry. In the case of Karymshina station, Figure 5, over the sea immediately south and east from Australia, and in the case of Marion station, Figure 7, over the North Sea, the transmission rate seems to decrease more slowly towards the ocean than towards the continent. To a lesser extent, similar asymmetry may be observed at Rothera, Halley and SANAE, Figure 6, although this may also be interpreted as an offset of the center of the transmission rate distribution from the conjugate point. A statistically stronger transmission rate of ocean lightning may be due to oceanic lightning having higher peak currents. We would not venture into interpreting any other apparent shapes in the transmission rate maps, as they can be sensitive to individual storm events, especially where average lightning activity is otherwise low, and can show slight changes from year to year, to be investigated in our followup study. The slight differences between the transmission rates at three closely separated stations on Figure 9 show the limits of our method.

In addition to listing the obtained maximal transmission rates at each station in Table 1), we plotted them on Figure 10. We note that the number of observable whistlers, and therefore the transmission rates are sensitive to the local noise, which may be different at each station, can vary over time, and is difficult to quantify. Nevertheless, a trend of transmission rates increasing with the stations' L-value is apparent, with only three outlier points. An explanation of the outliers may be that at these three stations, especially at Karymshina and Palmer, the VLF records generally show extremely good signal quality (low background noise), which possibly contributes to the detection of low amplitude whistlers by the AWDANet algorithm, translating into a higher total count and therefore also a higher transmission rate. This can only be confirmed through the laborious task of visually checking large periods of raw measurement at each station. Until whistler detection efficiencies are determined, values on Figure 10 should be taken with caution. The trend, however, may be explained by increased absorption of whistlers at lower latitudes due to the larger dip angle (Helliwell, 1965).

6 Conclusion

We present a method to identify the general location of lightning strokes that excite detectable whistlers at ground-based receivers. Our method also maps the geographic distribution of the lightning to whistler transmission rate. Our method is very general and can be applied to any dataset consisting of a whistler time series at a fixed location and a lightning database listing lightning times and locations. Our method produces results for even low number of whistlers (e.g. Eskdalemuir with $\sim 10^4$ traces, see Figure 8). We applied this procedure to whistler time series recorded at fifteen ground stations over twelve years. Our results confirm that at all of the fifteen locations the highest probability of lightning to produce a whistler detectable on the ground in the conjugate hemisphere is when the lightning is located at the geomagnetic conjugate point to the whistler observation station. This probability decreases with increasing distance from the conjugate point. In some cases, there is source lightning present over 3000 km from the conjugate point.

Our results are most consistent with the theory that whistlers detected on the ground propagated in a ducted mode through the plasmasphere and thus the whistler producing lightning strokes must cluster around the footprint of the ducts in the other hemisphere. This finding has implications for the importance of ground based VLF sources, whether natural or manmade, on the loss of radiation belt electrons. It also helps clarify the application of AWDANet observations to plasmaspheric monitoring, as the AWDANet reported whistler is likely to have passed through the plasmasphere on a duct that is rather local to the AWDANet station.

Our method has a significant potential to derive subsequent results. Having established the location of the source lightning, we can investigate how the transmission rates vary and what are they influenced by. It is possible to look at the variation of transmission rates as a function of time of day, season, ionospheric parameters and geomagnetic activity. Notably, our whistler database now covers more than one solar cycle, another time variable that may affect whistler transmission. It can also be of interest to see whether the transmission rate depends on the parameters of the lightning, e. g. peak current, cloud-to-ground versus intracloud lightning, etc. Similarly, we can look at transmission rates as a function of the parameters of the whistlers, such as whistler amplitude, propagation path L-value and plasmaspheric density obtained from inverted whistler traces. These questions are outside of the scope of this paper, but we intend to investigate these ideas and present them in a follow-up study.

Acknowledgments

AWDANet data is currently available from the leading authors upon request and will be accessible at http://plasmon.elte.hu/. The authors wish to thank the World Wide Lightning Location Network (http://wwlln.net), a collaboration among over 50 universities and institutions, for providing the lightning location data used in this paper. The research leading to these results received funding from the National Research, Development and Innovation Office of Hungary under grant agreements NN116408 and NN116446 and was supported by the UNKP-18-3 New National Excellence Program of the Ministry of Human Capacities of Hungary. We acknowledge NIIF for awarding us access to supercomputing resources based in Hungary at Debrecen. F. Darrouzet and S. Ranvier acknowledge BIRA-IASB (Royal Belgian Institute for Space Aeronomy), STCE (Solar-Terrestrial Center of Excellence) and BELSPO (Belgian Federal Science Policy Office) for their support.

References

Abarca, S. F., Corbosiero, K. L., & Galarneau, T. J. (2010, September). An evaluation of the Worldwide Lightning Location Network (WWLLN) using the National Lightning Detection Network (NLDN) as ground truth. *Journal of Geophysical Research (Atmospheres)*, *115*, D18206. doi: 10.1029/2009JD013411

Allcock, G. M. (1960, Nov 26). Propagation of whistlers to polar latitudes. *Nature*, *188*, 732. Retrieved from `http://dx.doi.org/10.1038/188732a0`

Antel, C., Collier, A. B., Lichtenberger, J., & Rodger, C. J. (2014, July). Investigating Dunedin whistlers using volcanic lightning. Geophys. Res. Lett., *41*, 4420-4426. doi: 10.1002/2014GL060332

Bortnik, J., Inan, U. S., & Bell, T. F. (2006, February). Temporal signatures of radiation belt electron precipitation induced by lightning-generated MR whistler waves: 2. Global signatures. *Journal of Geophysical Research (Space Physics)*, *111*, A02205. doi: 10.1029/2005JA011398

Carpenter, D. L. (1988, August). Remote sensing of the magnetospheric plasma by means of whistler mode signals. *Reviews of Geophysics*, *26*, 535-549. doi: 10.1029/RG026i003p00535

Carpenter, D. L., & Orville, R. E. (1989, July). The excitation of active whistler mode signal paths in the magnetosphere by lightning - Two case studies. J. Geophys. Res., *94*, 8886-8894. doi: 10.1029/JA094iA07p08886

Christian, H. J., Blakeslee, R. J., Boccippio, D. J., Boeck, W. L., Buechler, D. E., Driscoll, K. T., ... Stewart, M. F. (2003, January). Global frequency and distribution of lightning as observed from space by the Optical Transient Detector. *Journal of Geophysical Research (Atmospheres)*, *108*, 4005. doi: 10.1029/2002JD002347

Chum, J., Jiricek, F., Santolik, O., Parrot, M., Diendorfer, G., & Fiser, J. (2006, November). Assigning the causative lightning to the whistlers observed on satellites. *Annales Geophysicae*, *24*, 2921-2929. doi: 10.5194/angeo-24-2921-2006

Clilverd, M. A., Thomson, N. R., & Smith, A. J. (1992, August). Observation of two preferred propagation paths for whistler mode VLF signals received at a non-conjugate location. *Journal of Atmospheric and Terrestrial Physics*, *54*, 1075-1079. doi: 10.1016/0021-9169(92)90073-T

Collier, A. B., Bremner, S., Lichtenberger, J., Downs, J. R., Rodger, C. J., Steinbach, P., & McDowell, G. (2010, February). Global lightning distribution and whistlers observed at Dunedin, New Zealand. *Annales Geophysicae*, *28*, 499-513. doi: 10.5194/angeo-28-499-2010

Collier, A. B., Delport, B., Hughes, A. R. W., Lichtenberger, J., Steinbach, P., Öster, J., & Rodger, C. J. (2009, July). Correlation between global lightning and whistlers observed at Tihany, Hungary. *Journal of Geophysical Research (Space Physics)*, *114*, A07210. doi: 10.1029/2008JA013863

Collier, A. B., Hughes, A. R. W., Lichtenberger, J., & Steinbach, P. (2006, March). Seasonal and diurnal variation of lightning activity over southern Africa and correlation with European whistler observations. *Annales Geophysicae*, *24*, 529-542. doi: 10.5194/angeo-24-529-2006

Collier, A. B., Lichtenberger, J., Clilverd, M. A., Rodger, C. J., & Steinbach, P. (2011, March). Source region for whistlers detected at Rothera, Antarctica. *Journal of Geophysical Research (Space Physics)*, *116*, A03219. doi: 10.1029/2010JA016197

Gokani, S. A., Singh, R., Cohen, M. B., Kumar, S., Venkatesham, K., Maurya, A. K., ... Lichtenberger, J. (2015, August). Very low latitude (L = 1.08) whistlers and correlation with lightning activity. *Journal of Geophysical Research (Space Physics)*, *120*, 6694-6706. doi: 10.1002/2015JA021058

Helliwell, R. A. (1965). *Whistlers and related ionospheric phenomena.* Stanford: Stanford University Press.

Helliwell, R. A., Katsufrakis, J. P., & Trimpi, M. L. (1973, August). Whistler-induced amplitude perturbation in VLF propagation. J. Geophys. Res., *78*, 4679-4688. doi: 10.1029/JA078i022p04679

Holzworth, R. H., Winglee, R. M., Barnum, B. H., Li, Y., & Kelley, M. C. (1999, August). Lightning whistler waves in the high-latitude magnetosphere. J. Geophys. Res., *104*, 17369-17378. doi: 10.1029/1999JA900160

Hutchins, M. L., Holzworth, R. H., Brundell, J. B., & Rodger, C. J. (2012, December). Relative detection efficiency of the World Wide Lightning Location Network. *Radio Science*, *47*, RS6005. doi: 10.1029/2012RS005049

Lauben, D. S., Inan, U. S., & Bell, T. F. (2001, December). Precipitation of radiation belt electrons induced by obliquely propagating lightning-generated whistlers. J. Geophys. Res., *106*, 29745-29770. doi: 10.1029/1999JA000155

Lichtenberger, J., Clilverd, M. A., Heilig, B., Vellante, M., Manninen, J., Rodger, C. J., … Simon-Wedlund, M. (2013). The plasmasphere during a space weather event: first results from the plasmon project. *J. Space Weather Space Clim.*, *3*, A23. doi: 10.1051/swsc/2013045

Lichtenberger, J., Ferencz, C., Bodnár, L., Hamar, D., & Steinbach, P. (2008, December). Automatic Whistler Detector and Analyzer system: Automatic Whistler Detector. *Journal of Geophysical Research (Space Physics)*, *113*(A12), A12201. doi: 10.1029/2008JA013467

Lichtenberger, J., Ferencz, C., Hamar, D., Steinbach, P., Rodger, C. J., Clilverd, M. A., & Collier, A. B. (2010, December). Automatic Whistler Detector and Analyzer system: Implementation of the analyzer algorithm. *Journal of Geophysical Research (Space Physics)*, *115*, A12214. doi: 10.1029/2010JA015931

Morgan, M. G., & Allcock, G. M. (1956, January). Observations of Whistling Atmospherics at Geomagnetically Conjugate Points. Nature, *177*, 30-31. doi: 10.1038/177030a0

Ohta, K., & Hayakawa, M. (1990, March). The correlation of whistler occurrence rate at a low latitude with thunderstorm activity at its conjugate region and with solar activity. *Pure and Applied Geophysics*, *133*, 167-178. doi: 10.1007/BF00876709

Öster, J. (2009). Spatial correlation between lightning strikes and whistler observations. *South African Journal of Science*, *105*, 234-237.

Park, C. G. (1972). *Methods to determine electron concentrations in the magnetosphere from nose whistlers* (Technical report No. 3454-1). Stanford, California: Radioscience Laboratory, Stanford Electronics Laboratories, Stanford University.

Park, C. G., Carpenter, D. L., & Wiggin, D. B. (1978, July). Electron density in the plasmasphere - Whistler data on solar cycle, annual, and diurnal variations. J. Geophys. Res., *83*, 3137-3144. doi: 10.1029/JA083iA07p03137

Rao, M., Somayajulu, V. V., Dikshit, S. K., & Tantry, B. A. P. (1974, September). Low-latitude cutoff for whistlers observed on the ground. J. Geophys. Res., *79*, 3867-3869. doi: 10.1029/JA079i025p03867

Rodger, C., Brundell, J., Hutchins, M., & Holzworth, R. (2014). The world wide lightning location network (WWLLN): Update of status and applications. In *XXXIth URSI General Assembly and Scientific Symposium (URSI GASS).*

Rodger, C. J., Brundell, J. B., Holzworth, R. H., & Lay, E. H. (2009, April). Growing Detection Efficiency of the World Wide Lightning Location Network. In *American Institute of Physics Conference Series* (Vol. 1118, p. 15-20). doi: 10.1063/1.3137706

Rodger, C. J., Enell, C.-F., Turunen, E., Clilverd, M. A., Thomson, N. R., & Verronen, P. T. (2007, August). Lightning-driven inner radiation belt energy deposition into the atmosphere: implications for ionisation-levels and neutral chemistry. *Annales Geophysicae*, *25*, 1745-1757. doi: 10.5194/angeo-25-1745-2007

Rodger, C. J., Lichtenberger, J., McDowell, G., & Thomson, N. R. (2009, April). Automatic whistler detection: Operational results from New Zealand. *Radio Science*, *44*, RS2004. doi: 10.1029/2008RS003957

Rodger, C. J., McCormick, R. J., & Clilverd, M. A. (2004, May). Testing the importance of precipitation loss mechanisms in the inner radiation belt. Geophys. Res. Lett., *31*, L10803. doi: 10.1029/2004GL019501

Rodger, C. J., Werner, S., Brundell, J. B., Lay, E. H., Thomson, N. R., Holzworth, R. H., & Dowden, R. L. (2006, December). Detection efficiency of the VLF World-Wide Lightning Location Network (WWLLN): initial case study. *Annales Geophysicae*, *24*, 3197-3214. doi: 10.5194/angeo-24-3197-2006

Smith, R. L. (1961, November). Propagation Characteristics of Whistlers Trapped in Field-Aligned Columns of Enhanced Ionization. J. Geophys. Res., *66*, 3699-

3707. doi: 10.1029/JZ066i011p03699

Smith, R. L., Helliwell, R. A., & Yabroff, I. W. (1960, March). A Theory of Trapping of Whistlers in Field-Aligned Columns of Enhanced Ionization. J. Geophys. Res., *65*, 815. doi: 10.1029/JZ065i003p00815

Storey, L. R. O. (1953, July). An Investigation of Whistling Atmospherics. *Philosophical Transactions of the Royal Society of London Series A*, *246*, 113-141. doi: 10.1098/rsta.1953.0011

Thébault, E., Finlay, C. C., Beggan, C. D., Alken, P., Aubert, J., Barrois, O., ... Zvereva, T. (2015, May). International Geomagnetic Reference Field: the 12th generation. *Earth, Planets, and Space*, *67*, 79. doi: 10.1186/s40623-015-0228-9

Trakhtengerts, V. Y., Rycroft, M. J., Nunn, D., & Demekhov, A. G. (2003, March). Cyclotron acceleration of radiation belt electrons by whistlers. *Journal of Geophysical Research (Space Physics)*, *108*, 1138. doi: 10.1029/2002JA009559

Virts, K. S., Wallace, J. M., Hutchins, M. L., & Holzworth, R. H. (2013, September). Highlights of a New Ground-Based, Hourly Global Lightning Climatology. *Bulletin of the American Meteorological Society*, *94*, 1381-1391. doi: 10.1175/BAMS-D-12-00082.1

Vodinchar, G. M., Sivokon', V. P., Cherneva, N. V., Shevtsov, B. M., & Malysh, E. A. (2014). Possible effects of the lightning centers in whistler rates in Kamchatka. *Bulletin KRASEC. Phys. & Mat. Sci.*, *9*(2), 39-47. doi: 10.18454/2313-0156-2014-9-2-39-47

Yoshino, T. (1976, September). Low-latitude whistlers and cloud distributions in the conjugate area. J. Geophys. Res., *81*, 4793-4796. doi: 10.1029/JA081i025p04793

Záhlava, J., Němec, F., Santolík, O., Kolmašova, I., Hospodarsky, G. B., Parrot, M., ... Kletzing, C. (2018, August). Longitudinal Dependence of Whistler Mode Electromagnetic Waves in the Earth's Inner Magnetosphere. *Journal of Geophysical Research (Space Physics)*, *123*, 6562-6575. doi: 10.1029/2018JA025284

Zheng, H., Holzworth, R. H., Brundell, J. B., Jacobson, A. R., Wygant, J. R., Hospodarsky, G. B., ... Bonnell, J. (2016, March). A statistical study of whistler waves observed by Van Allen Probes (RBSP) and lightning detected by WWLLN. *Journal of Geophysical Research (Space Physics)*, *121*, 2067-2079. doi: 10.1002/2015JA022010

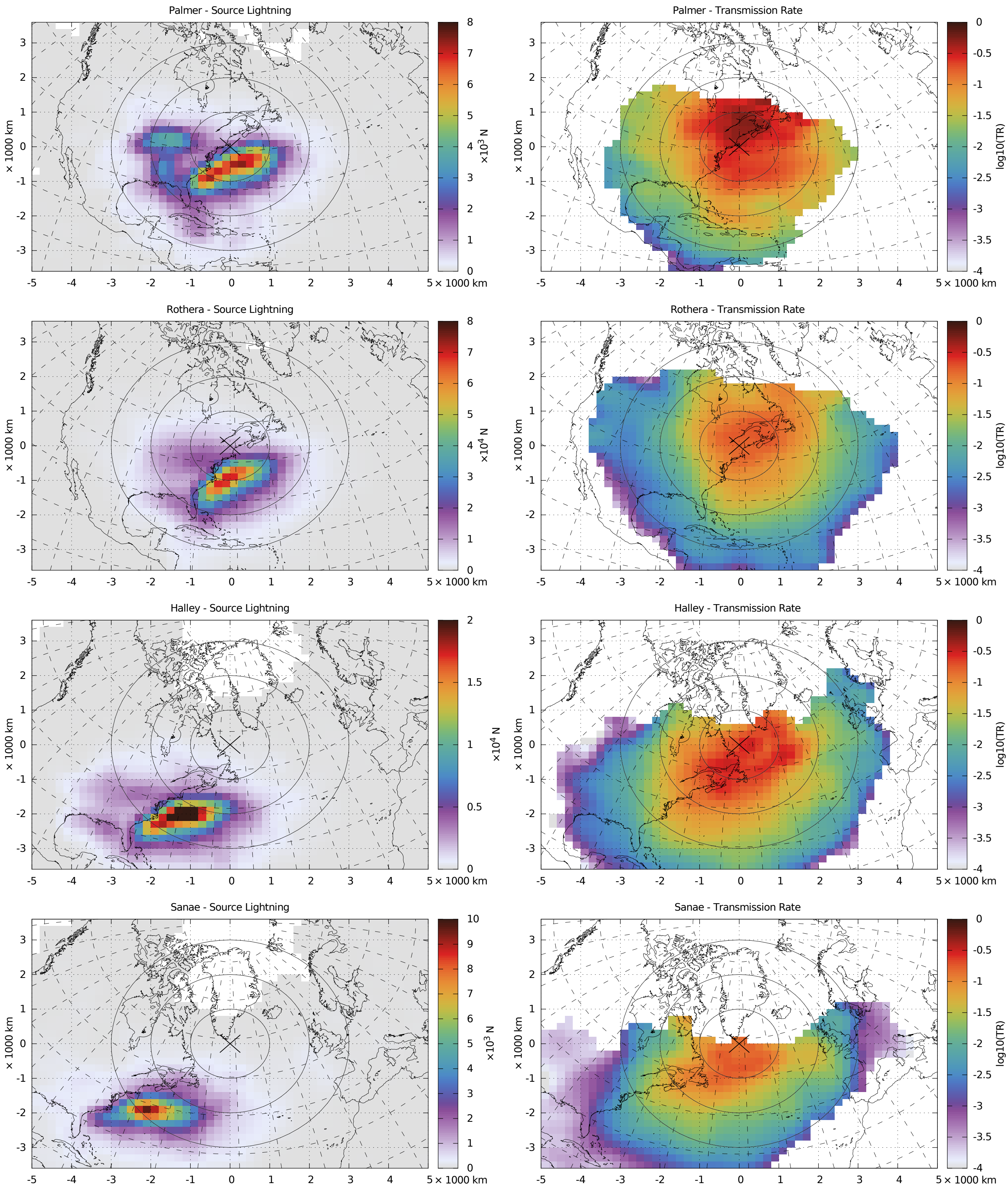

402 **Figure 6.** Regional distribution of source lightning and transmission rate for whistlers de-
403 tected at stations in West Antarctica

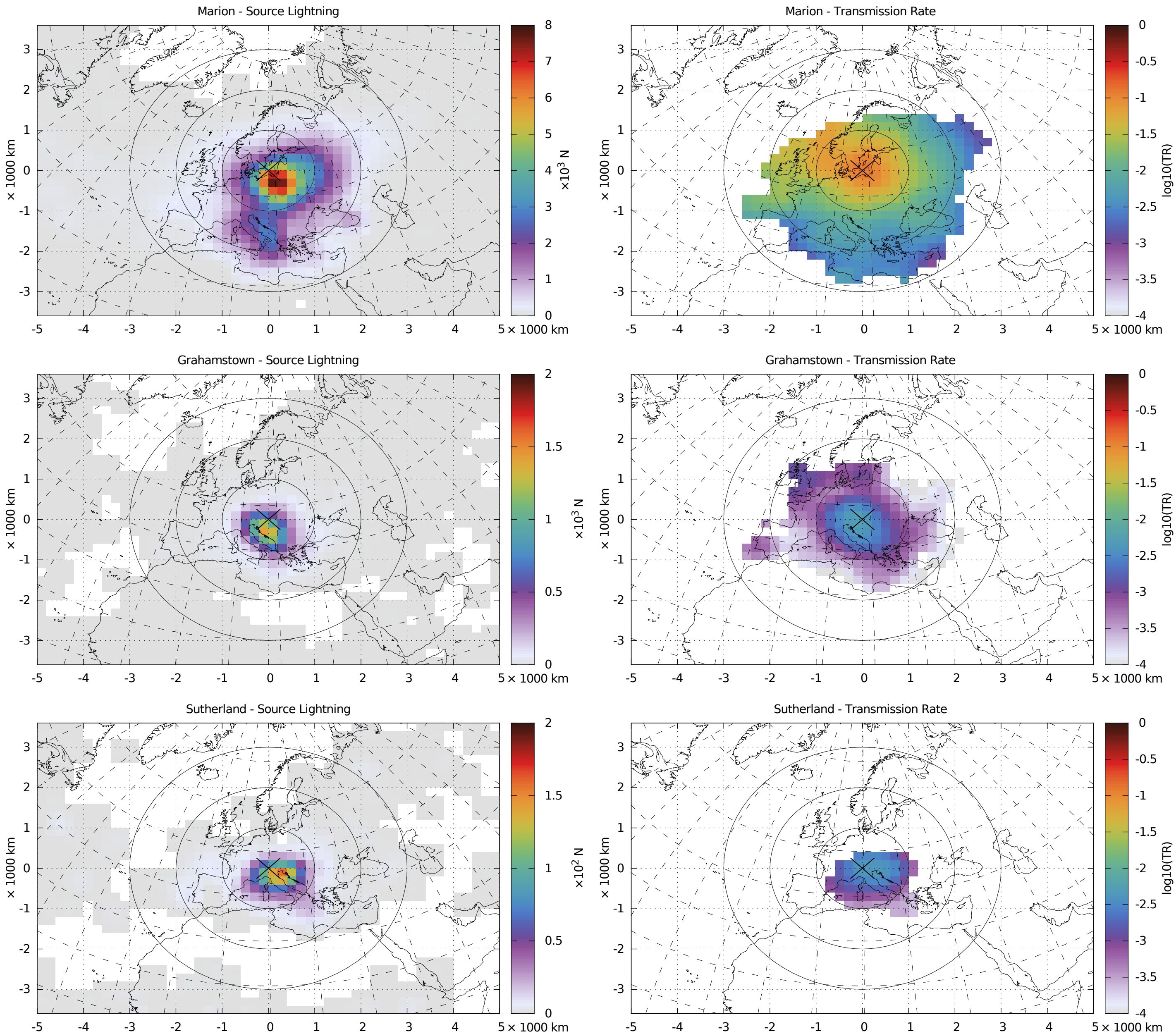

404 **Figure 7.** Regional distribution of source lightning and transmission rate for whistlers de-
405 tected in southern Africa.

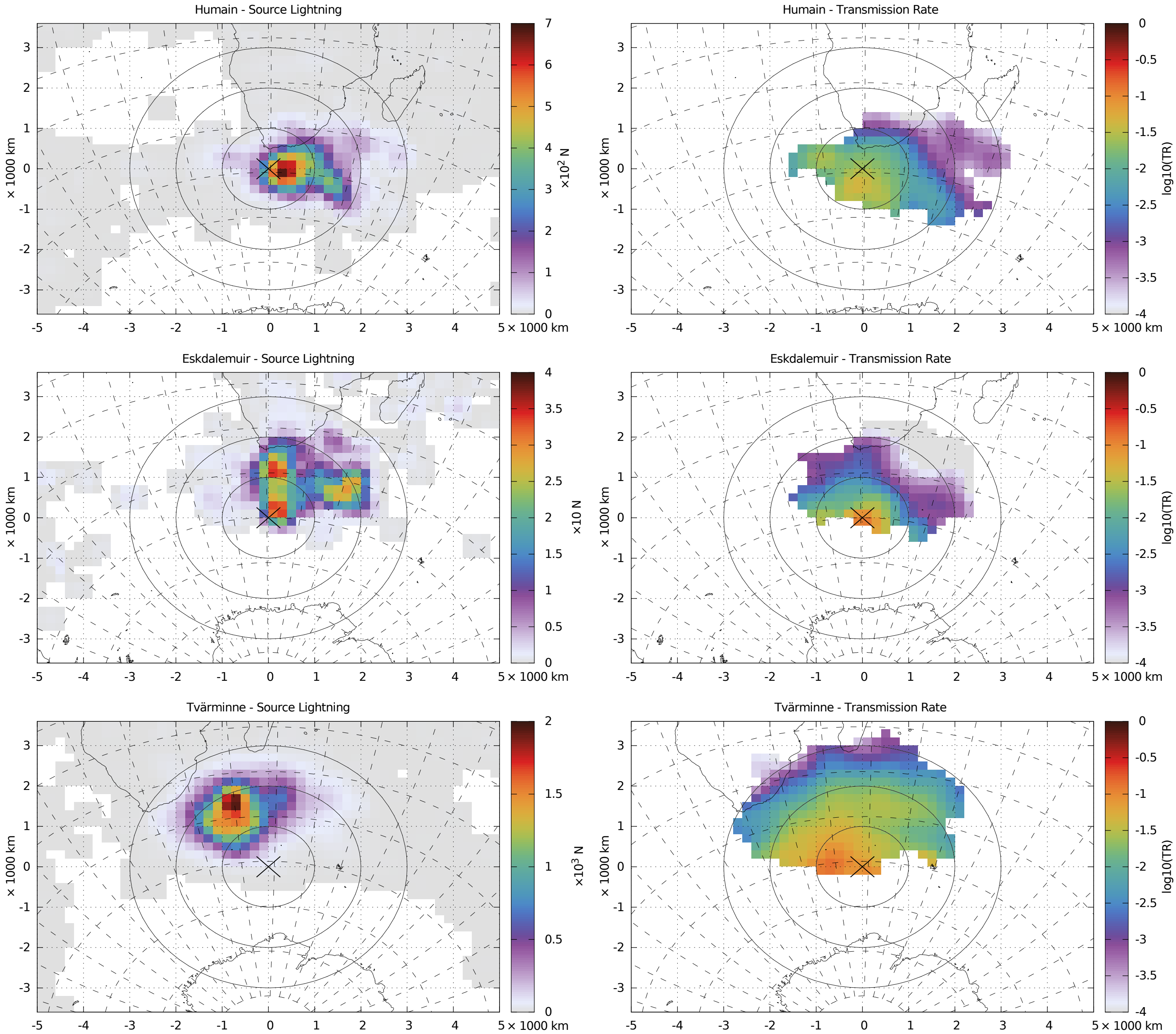

406 **Figure 8.** Regional distribution of source lightning and transmission rate for whistlers de-
407 tected at European stations.

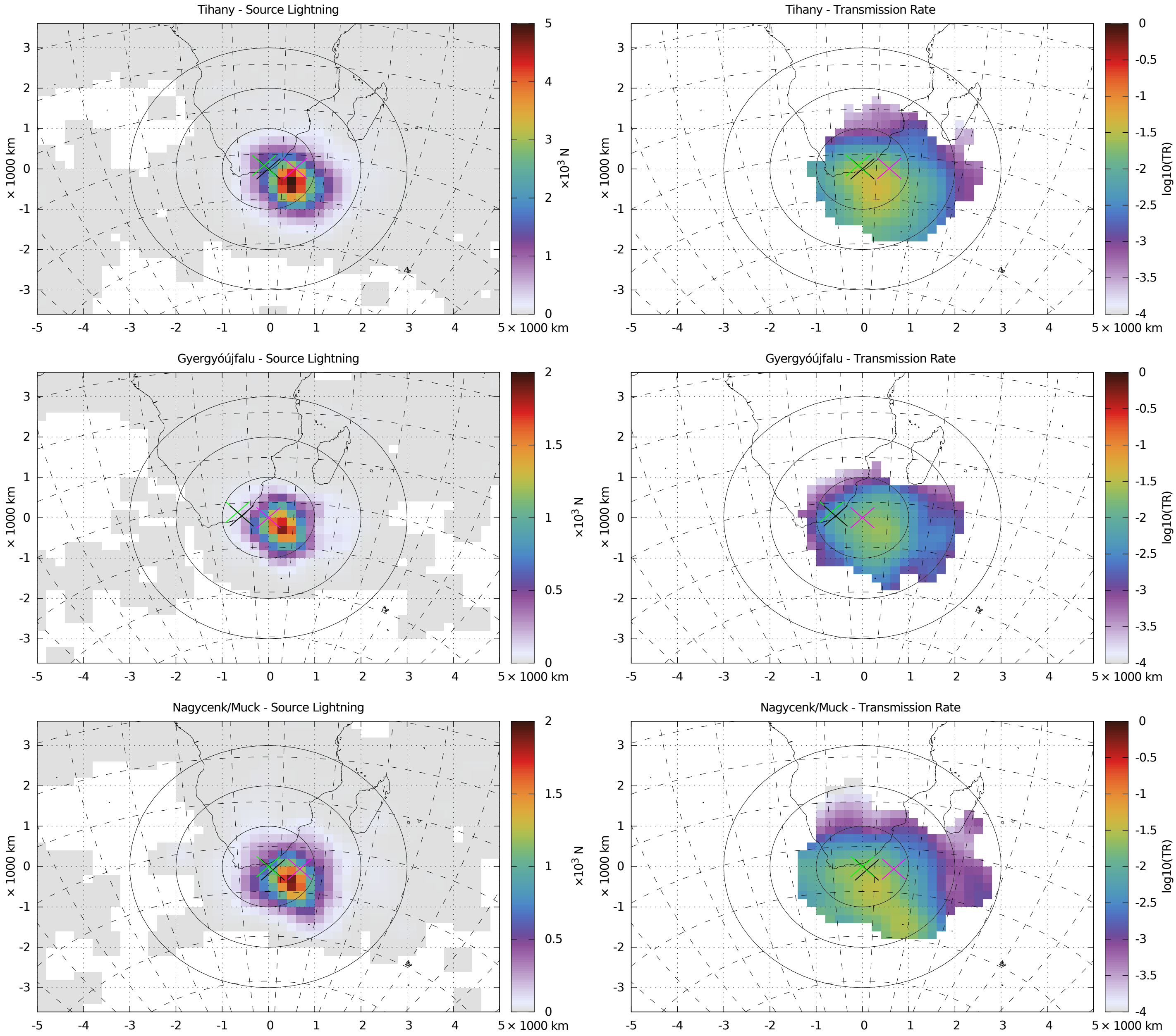

408 **Figure 9.** Regional distribution of source lightning and transmission rate whistlers detected at
409 the European stations of Tihany (black cross), Nagycenk/Muck (blue cross) and Gyergyóújfalu
410 (magenta cross).

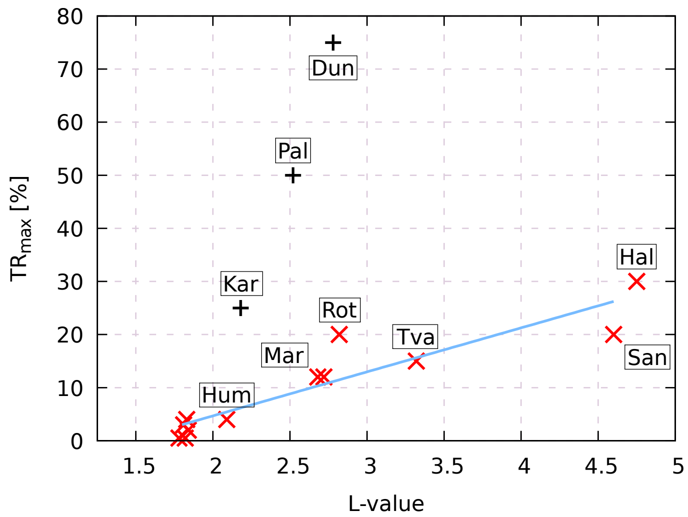

Figure 10. A comparison of the obtained maximal transmission rates at each station with the L-value of the given station (see Table 1). A trend of transmission rates increasing with L-values is apparent, with the exception of three points (Karymshina, Dunedin and Palmer), which we considered outliers and marked with black points. The blue line is a straight line fitted to the non-outlier points.